



Diurnal dependence of ELF/VLF hiss and its relation to chorus at $L = 2.4$

D. I. Golden,¹ M. Spasojevic,¹ and U. S. Inan¹

Received 24 November 2008; revised 20 February 2009; accepted 3 March 2009; published 21 May 2009.

[1] We present the observation and analysis of all very low frequency (0.3–10 kHz) chorus and hiss emissions observed at Palmer Station, Antarctica ($L = 2.4$), from January through October 2003, near the peak of the most recent solar cycle. We classify three separate categories of emissions: chorus occurring without the presence of hiss (“chorus only”), hiss occurring without the presence of chorus (“hiss only”), and chorus and hiss occurring simultaneously (“chorus with hiss”). We find that observed chorus only and chorus with hiss emissions are confined to the dawn sector, below 6 kHz in frequency. Observed hiss only emissions are confined to the dusk sector, below 4 kHz in frequency. We conclude that there are at least two distinct types of hiss observed at Palmer Station: hiss that is observed with chorus in the dawn sector and hiss that is observed without chorus in the dusk sector. The correspondence of dawn chorus with dawn hiss suggests that these two emissions are strongly related to each other, while the frequency spectrum and local time distribution of dusk hiss, coupled with the absence of simultaneous chorus, suggest that dusk hiss may be generated by terrestrial lightning.

Citation: Golden, D. I., M. Spasojevic, and U. S. Inan (2009), Diurnal dependence of ELF/VLF hiss and its relation to chorus at $L = 2.4$, *J. Geophys. Res.*, 114, A05212, doi:10.1029/2008JA013946.

1. Introduction

[2] Extremely low frequency/very low frequency (ELF/VLF) chorus and hiss are two common types of electromagnetic waves found in the Earth’s magnetosphere. Both are thought to play major roles in the acceleration [Horne *et al.*, 2003, 2005] and loss [Lyons *et al.*, 1972; Lyons and Thorne, 1973; Abel and Thorne, 1998] of energetic electrons in the Earth’s radiation belts. The extensive review papers available for both chorus [Sazhin and Hayakawa, 1992; Santolik, 2008] and hiss [Hayakawa and Sazhin, 1992] are indicative of the amount of attention that these waves have warranted in recent and past years.

[3] Magnetospheric chorus (hereinafter referred to as “chorus”) is an ELF/VLF emission, originating outside the plasmasphere, typically appearing below ~ 10 kHz [Helliwell, 1965]. Chorus is characterized by a closely spaced series of semicoherent discrete tones, usually rising in frequency with time, at a rate of up to a few kHz/sec. Numerous studies performed using ground-based [Allcock, 1957; Pope, 1957, 1960] and space-based [Burtis and Helliwell, 1976; Meredith *et al.*, 2001; Tsurutani and Smith, 1977] receivers have shown that, although the local time of maximal chorus occurrence increases with increasing L shell, chorus is nonetheless primarily confined to the dawn and day sectors at all L shells. Chorus occurrence is a strong function of geomagnetic activity and substorms [Tsurutani

and Smith, 1974; Burtis and Helliwell, 1976; Meredith *et al.*, 2001].

[4] Several varieties of hiss permeate the magnetosphere. All varieties of hiss are composed of incoherent, unstructured emissions. Naming conventions for the different varieties of hiss are occasionally contested, which is not surprising considering the preponderance of ground and space-based observations of hiss, often with different conclusions.

[5] One type of hiss of which there is not currently much nomenclature dispute is auroral hiss. As its name implies, auroral hiss appears near the auroral zone, and has a frequency range that can extend up to several hundred kHz [e.g., Jørgensen, 1968; Makita, 1979]. We will not discuss auroral hiss in this paper.

[6] Four other distinct types of ELF/VLF hiss exist: plasmaspheric hiss, exo-hiss, ELF hiss and midlatitude hiss. We make mention of these different types of hiss emissions here in order to contrast their definitions with the hiss emissions observed at Palmer later in this paper.

[7] “Plasmaspheric hiss” is an emission that is seen exclusively within the plasmasphere. Plasmaspheric hiss peaks in amplitude slightly below 1 kHz, and can extend up to ~ 3 kHz. Satellite observations have found that plasmaspheric hiss occurs primarily in the day and dusk sectors, although the amplitude of the hiss and the specific L shells and local times of maximum observation are strong functions of geomagnetic activity [Parady *et al.*, 1975; Meredith *et al.*, 2004]. It is supposedly never observed on the ground [Sonwalkar, 1995; Santolik *et al.*, 2006] owing to theoretical considerations of magnetospheric reflection near the local lower hybrid resonance frequencies [Thorne

¹Space, Telecommunications, and Radioscience Laboratory, Stanford University, Stanford, California, USA.

and Kennel, 1967] and the low-frequency cutoff between the proton and helium gyrofrequencies [Gurnett and Burns, 1968]. Although Hayakawa *et al.* [1985] claimed to have made ground observations of plasmaspheric hiss, the frequency range (mostly above ~ 1.5 kHz) was generally more in line with that of midlatitude hiss (see below). Kleimenova *et al.* [1976] made ground observations of morning hiss at 400 Hz during periods of low geomagnetic activity level, but stated that this could not be plasmaspheric hiss in light of the above cited work by Thorne and Kennel [1967] and Gurnett and Burns [1968].

[8] Two separate types of hiss, whose frequency spectrum resembles that of plasmaspheric hiss, are seen at medium latitudes outside of the plasmasphere, and are known either as “exo-hiss” or “ELF hiss.” ELF hiss and exo-hiss share similar frequencies and latitudes of observation, but are differentiated primarily by their diurnal occurrence and theorized generation methods. Exo-hiss is believed to be the result of plasmaspheric hiss leaking out of the plasmasphere [Thorne *et al.*, 1973; Bortnik *et al.*, 2008], and appears primarily in the afternoon sector. ELF hiss appears primarily on the dayside [Russell *et al.*, 1972; Meredith *et al.*, 2004; Santolik *et al.*, 2006], and although the actual origin of ELF hiss is controversial, it is generally agreed to be caused by emissions generated equatorially outside of the plasmopause, propagating to low altitudes [Santolik *et al.*, 2006; Bortnik *et al.*, 2008]. It should be cautioned that the term “ELF hiss” can be misleading, particularly since plasmaspheric hiss and exo-hiss also appear in the ELF frequency range. In this paper, we use the term “ELF hiss” strictly to mean dayside hiss in the ELF range that has originated from an exo-plasmaspheric equatorial source.

[9] “Midlatitude hiss” is a VLF emission that is generally observed on the ground and low-altitude satellites with an intensity and occurrence peak between 50° and 65° invariant latitude. Higher-altitude satellites have also seen midlatitude hiss at latitudes everywhere from the equator to subauroral latitudes [Taylor and Gurnett, 1968; Dunckel and Helliwell, 1969]. Midlatitude hiss correlates well with geomagnetic activity, increasing in intensity and occurrence, and decreasing in L shell as Kp increases. Midlatitude hiss can generally extend from ~ 2 to 10 kHz, though its bandwidth and center frequency is variable [Hayakawa and Sazhin, 1992; Sonwalkar, 1995]. It is worth noting that the primary observational difference between midlatitude hiss and the other types of hiss discussed here is the observed frequency range ($f \gtrsim 2$ kHz for midlatitude hiss versus $f \lesssim 3$ kHz for plasmaspheric, ELF and exo-hiss, with an overlap between ~ 2 – 3 kHz).

[10] Outwardly, chorus and hiss have very different properties, and often occur in different local times, at different frequencies and in different parts of the magnetosphere, particularly during storms [Hayakawa *et al.*, 1975b, 1977]. However, they do have overlapping frequency bands, and are also often observed simultaneously [Dunckel and Helliwell, 1969; Koons, 1981; Parrot *et al.*, 2004; Santolik *et al.*, 2006]. In particular, Cornilleau-Wehrlin *et al.* [1978] made observations of chorus and hiss with the GEOS spacecraft at high altitudes ($\geq 6 R_e$) and low geomagnetic activity levels ($K_p < 3^-$), demonstrating that “chorus with hiss” is the dominant emission in this region.

[11] Many attempts have been made to explain the connections between chorus and hiss. Koons [1981] suggested that hiss emissions may set up a suitable electron anisotropy for the generation of chorus. Electrons, phase-bunched owing to the hiss emissions, then generate chorus emissions as they move adiabatically along magnetic field lines. This hypothesis was supported experimentally via experiments by Helliwell *et al.* [1986], during which hiss-like incoherent noise, radiated by the Siple transmitter in Antarctica, was observed to trigger discrete emissions. An alternate hypothesis for the chorus-hiss connection is that hiss is generated by overlapping chorus emissions, whose frequency-time structures have become sufficiently diffuse that they eventually appear hiss-like to observers [Santolik *et al.*, 2006; Bortnik *et al.*, 2008].

[12] Parrot *et al.* [2004] specifically made note of hiss emissions on the Cluster satellites that showed signs of discrete structure, the first suggestions of a VLF Archaeopteryx: an emission that bridges the gap between chorus and hiss. Santolik *et al.* [2006] took this idea further by using wavelet techniques on data from the Freja and DEMETER satellites. This allowed them to discover discrete chorus-like structure hidden within emissions that were ostensibly ELF hiss on traditional spectrograms; they referred to these emissions as “structured hiss.” They used ray tracing techniques to show that emissions generated in the equatorial region outside of the plasmopause, given the proper initial wavenormal angles, could penetrate to very low altitudes (at high latitudes), and possibly to the ground. Stating that “the origin and source region of ‘structured hiss’ and ducted chorus are most probably the same,” Santolik *et al.* [2006] concluded by saying that these observations were “consistent with the hypothesis that the frequently observed dayside ELF hiss is just the low-altitude manifestation of . . . whistler mode chorus.”

[13] Chum and Santolik [2005] used ray tracing to show that chorus waves, generated equatorially at high altitudes, could penetrate the plasmasphere under certain circumstances and potentially become trapped there. Bortnik *et al.* [2008] expanded on these results via a more extensive and rigorous ray tracing study, which showed that chorus waves could penetrate into the plasmasphere and remain there via magnetically reflecting for tens of seconds before being damped. By showing that this phenomenon could occur both on the dayside and nightside (albeit at reduced efficiencies on the nightside), Bortnik *et al.* [2008] concluded on the basis of this study that “chorus waves are the dominant source of plasmaspheric hiss.”

[14] An alternate hypothesis is that lightning is a major source of plasmaspheric hiss [Sonwalkar and Inan, 1989; Draganov *et al.*, 1992]. Recent work by Green *et al.* [2005] and Meredith *et al.* [2006] has shown experimental data highlighting the correlation of terrestrial lightning rates with certain frequencies of hiss. Although they disagreed on the exact frequencies, Green *et al.* [2005] and Meredith *et al.* [2006] both concluded that lightning may be a dominant source of hiss above either 500 Hz or 2 kHz, respectively, although Meredith *et al.* [2006] did note that the lower-frequency, non-lightning-associated hiss, being more intense than the lightning-associated variety, is a more important loss mechanism for relativistic electrons between $2 < L < 3$.

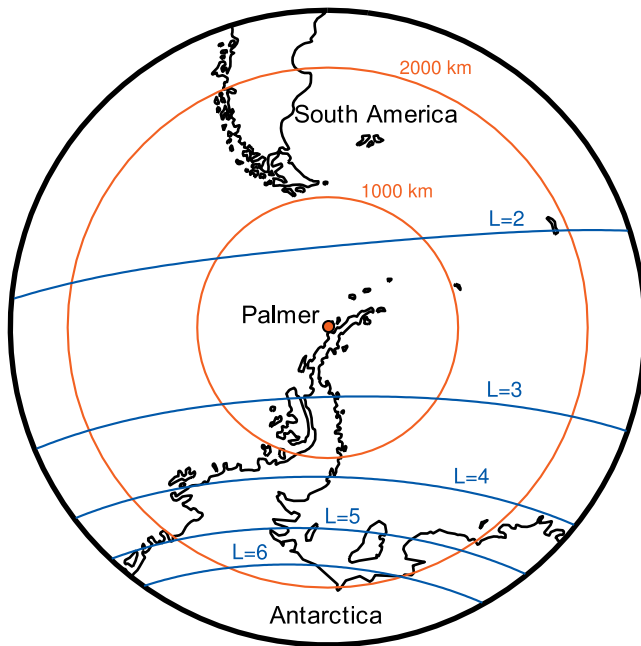


Figure 1. Palmer station, located near the tip of the Antarctic peninsula ($L = 2.4$, 50°S magnetic latitude).

[15] This study presents ten months of data recorded on the ground with Stanford University’s ELF/VLF broadband receiver at Palmer Station, Antarctica. The preponderance of ELF/VLF emissions observed daily at Palmer (chorus and hiss are each observed on more than 50% of days), coupled with modern analysis techniques, allow us to test the above mentioned current theories of hiss source mechanisms.

[16] It is important to note that, although ground-based measurements have several advantages over in situ space-based measurements, such as the ability to consistently observe a single L shell, and greatly increased data rates, they are only capable of sampling the portion of the magnetospheric waves that are able to penetrate to low altitudes and through the ionosphere [see, e.g., *Sonwalkar*, 1995, pp. 424–425]. This may include either waves that have propagated such that their wavenormals are within the transmission cone at the ionospheric boundary [*Helliwell*,

1965, section 3.7], or waves that have scattered from low-altitude meter-scale density irregularities [*Sonwalkar and Harikumar*, 2000]. Thus we would not expect all types of waves observed in space to be observed on the ground, and we will interpret our results accordingly.

2. Experimental Methodology

[17] Data were collected over the course of the year 2003 with the Stanford University ELF/VLF receiver at Palmer Station, Antarctica. Palmer Station is located on Anvers Island, near the tip of the Antarctic peninsula (Figure 1), at 64.77°S , 64.05°W , with IGRF geomagnetic parameters of $L = 2.4$, 50°S geomagnetic latitude. The Palmer VLF receiver records broadband VLF data at 100 kilosamples per second using two cross-loop magnetic field antennas, with 96 dB of dynamic range sensitivity. This analysis uses the North/South channel exclusively, it being the less subjectively noisy of the two channels; this has the additional effect of focusing Palmer’s viewing area more tightly to its magnetic meridian than if we made use of both channels. Data products used in this study are 3-min broadband data files, beginning every 15 min at 5, 20, 35 and 50 min past the hour, 24 h per day.

2.1. Emission Selection Criteria

[18] For each day of this study (1 January through 31 October 2003), we generate a 24-h combined synoptic spectrogram. These synoptic spectrograms consist of 96 5-s spectrograms stitched together horizontally, in the same format as in the work of *Spasojevic and Inan* [2005]. An example of this type of plot is shown in Figure 2. Emissions with amplitudes greater than $0.1 \text{ fT}/\sqrt{\text{Hz}}$ ($-20 \text{ dB-fT}/\sqrt{\text{Hz}}$) are visually located from these plots via their aberration from the blue background, below the frequency of the lightning-generated sferic impulses.

[19] Potential emissions are scrutinized via a higher resolution spectrogram. For the purposes of this study, without making any a priori assumptions about their generation regions, we characterize emissions solely on the basis of their observed spectral properties, irrespective of their local time or frequency characteristics. Emissions with incoherent spectral properties that do not exhibit any fine structure are labeled as hiss. Emissions that have obvious “chorus-like” characteristics, such as fine structure and

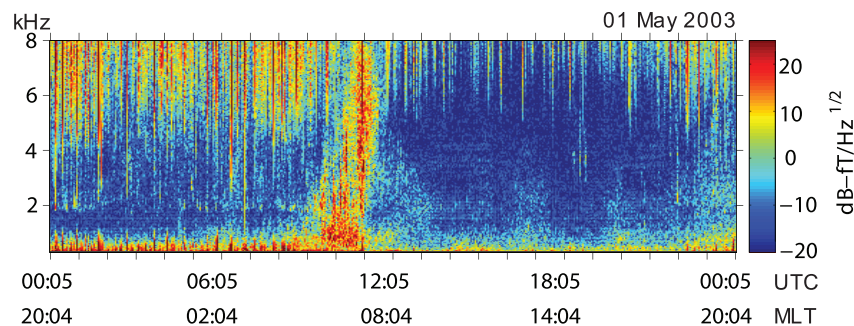


Figure 2. A 24-h VLF spectrogram from Palmer. This view is created by horizontally combining 96 separate 5-s spectrograms, each 15 min apart from each other. This particular 24-h spectrogram from 1 May 2003 shows one of the most intense emissions observed in 2003, consisting of varying forms of chorus and hiss from approximately 0800 to 1300 UTC (0359 to 0859 MLT).

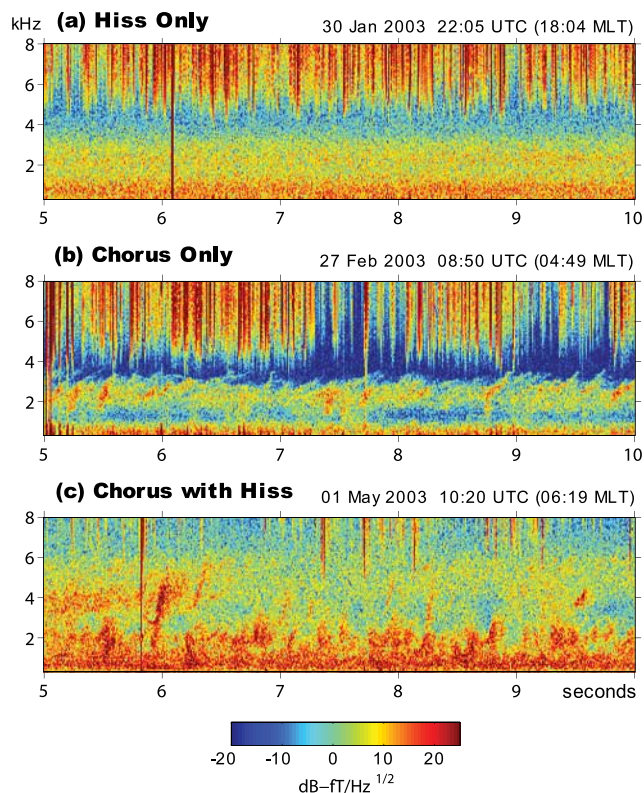


Figure 3. Examples of different emission types. (a) “Hiss only” is characterized by incoherent, unstructured emissions with no discrete elements, (b) “chorus only” consists of closely spaced, discrete tones, usually rising in frequency, and (c) “chorus with hiss” is a combination of the other two emissions.

rising tones, whose structure does not resemble that of multiply-hopping whistlers, are labeled as chorus. Often, chorus and hiss are seen simultaneously, in the form of multiple bands of emissions that may separately resemble chorus, hiss, or combinations of the two (such as the “structured hiss” from *Santolik et al.* [2006]). We consider these emissions separately, and refer to them as “chorus with hiss.”

[20] Throughout the course of this study, we refer to these three emission types separately as “hiss only,” “chorus only” and “chorus with hiss.” Examples of these three emissions can be seen in Figure 3. During this study, over the course of the 304 days for which we have valid data, we observed “hiss only” on 70% of days, “chorus only” on 30% of days and “chorus with hiss” on 36% of days.

2.2. Cumulative Spectrograms

[21] In order to visualize the entire year’s worth of emissions simultaneously, we use a “cumulative spectrogram” plot. This plot consists of the sum of all of the emissions of a given type, in spectrogram form. Technically, the cumulative spectrogram is generated as follows:

[22] 1. The emission database is constructed via the method outlined in section 2.1. The emission database is a list of emissions with the following properties: emission type (one of “chorus only,” “hiss only” or “chorus with hiss”), start time, end time, lower frequency cutoff, upper frequency cutoff.

[23] 2. For each emission window (bounded by the start and end times, and the lower and upper cutoff frequencies), the amplitude in dB of the spectrogram for that day, within those bounds, is added to the cumulative spectrogram plot.

[24] 3. The resulting spectrogram, which consists of the sum of the emissions from individual spectrograms, is then divided by 304, the number of days for which we have data. This results in a spectrogram of “average intensity.”

[25] The cumulative spectrogram is effectively the product, spectrogram-wise, of the occurrence rate of a given emission type with the average amplitude of that emission type, as illustrated in Figure 4.

3. Occurrence Characteristics

3.1. Local Time and Frequency

[26] Figure 5 shows separate cumulative spectrograms for each emission type. Consistent with previous studies of chorus [e.g., *Storey*, 1953; *Maeda*, 1962], “chorus only” emissions are observed exclusively in the dawn sector, from approximately 0400 to 0900 magnetic local time (MLT). “Chorus with hiss” emissions are observed at the same local time as “chorus only” emissions, but tend to be more common, and usually extend up to higher frequencies. “Chorus with hiss” emissions most commonly consist of a lower frequency band of chorus-like emission and an upper frequency band of hiss-like emission, though this is not always the case. Thus, the lower frequencies (below ~ 2 kHz) in the “chorus with hiss” cumulative spectrogram of Figure 5c are primarily chorus, while the higher frequencies are primarily hiss. The fact that “chorus only” and “chorus with hiss” emissions are seen at the same local times strongly suggests that their generation may be intimately related.

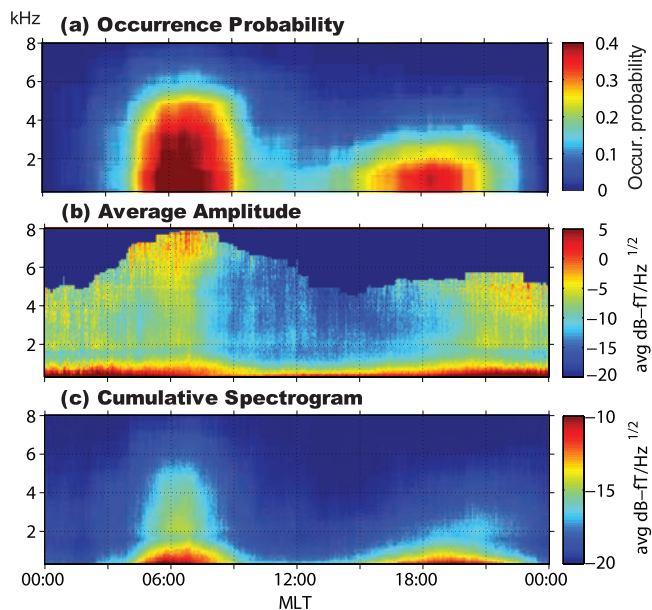


Figure 4. Cumulative spectrogram generation procedure. (a) The occurrence rate of a given emission is multiplied by (b) the average amplitude of the emission in dB, to give (c) an “average emission amplitude,” weighted by occurrence rate. This example shows plots for all emission types combined.

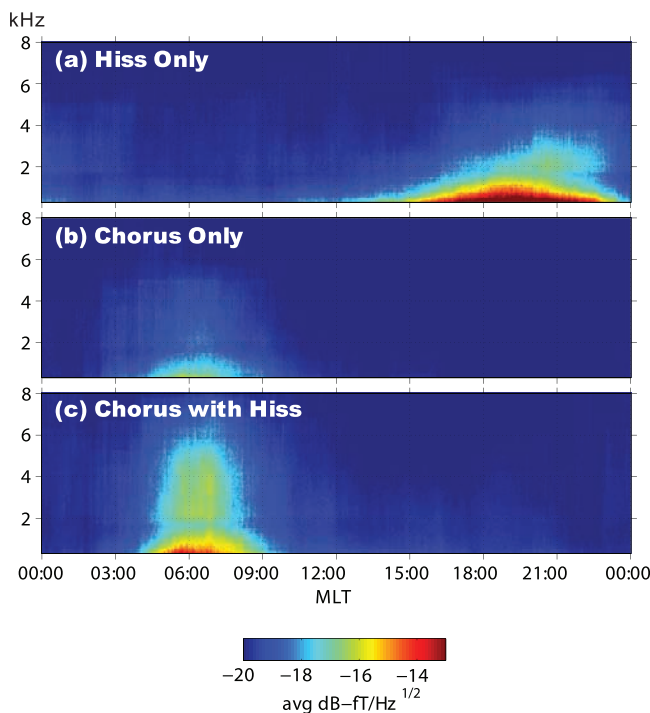


Figure 5. Cumulative spectrograms of (a) “hiss only” (408 events), (b) “chorus only” (99 events), and (c) “chorus with hiss” (151 events). “Hiss only” emissions are seen exclusively in the dusk sector, primarily below ~ 1.7 kHz, though they can extend up to ~ 4 kHz. “Chorus only” and “chorus with hiss” emissions appear exclusively in the dawn sector. The lack of emissions in the noon sector may be an ionospheric effect, but the lack of emissions in the midnight sector is almost definitely a true absence of low-altitude emissions.

Indeed, when characterizing the emissions, the authors found a continuum of emission types in between “chorus only” and “chorus with hiss” (i.e., varying amounts of structure in “structured hiss”).

[27] “Hiss only” emissions are observed exclusively in the dusk sector, from 1400 to 2300 MLT. This is similar to observations by other ground-based sites of similar L shells, although, in contrast to this study, *Laaspere et al.* [1964] also found a second maximum of hiss in the morning at North American stations at similar latitudes to Palmer, namely, Washington, D. C., ($L = 2.5$) and Dartmouth College ($L = 3.1$). *Hayakawa et al.* [1975a] found a similar double-peaked distribution at Moshiri, Japan ($L = 1.6$). This is possibly attributable to their characterizing as “hiss” what we determine to be “chorus with hiss” in the morning.

[28] Using data from the GEOS spacecraft at high radial distances ($\geq 6 R_e$), *Cornilleau-Wehrin et al.* [1978] also saw a majority of “chorus with hiss” emissions (with chorus as the greater amplitude emission) in the morning, suggesting that “chorus with hiss” emissions originate at high altitudes outside of the plasmapause, just as “chorus only” emissions do. In contrast to this study, they saw very few hiss emissions without accompanying chorus, but this is readily explained by the fact that the study was limited to satellite

radial distances greater than $6R_e$, which is outside the source region of hiss [*Meredith et al.*, 2004].

[29] Conspicuous in their absence are emissions in the noon sector and midnight sector. Using data from the Ogo 5 satellite [*Tsurutani and Smith*, 1977] showed that the L shell of maximal chorus occurrence increases from postmidnight to postdawn as a result of drift shell splitting, which is one reason why chorus would be unlikely to be seen at Palmer’s L shell outside of the dawn sector. Additionally, ionospheric absorption is a maximum during the daytime, owing to the increased electron density from solar radiation [e.g., *Helliwell*, 1965, Figure 3–35], which may have the net result of preventing magnetospheric emissions from reaching middle and low latitudes on the ground, regardless of their originating L shell. In the midnight sector, measurements using the CRRES satellite by *Meredith et al.* [2001, 2004] found a minimum of chorus at low altitudes and plasmaspheric hiss at all altitudes, respectively, so it is likely that the absence of emissions at Palmer in the midnight sector represent a true lack of emissions in the magnetosphere at low altitudes.

[30] “Chorus only” and “chorus with hiss” intensities gradually fall off as frequency increases from 300 Hz (the lowest frequency of these measurements) to around 6 kHz, with a noticeable discontinuity in intensity near 1.7 kHz. This discontinuity is due to the lower cutoff of the transverse electric (TE) mode in the Earth-Ionosphere (E-I) waveguide; below this cutoff, the transverse electromagnetic (TEM) mode dominates, with attenuation coefficient increasing with increasing frequency. This discontinuity is also visible at ~ 1.7 kHz for “hiss only” for the same reason.

[31] Below ~ 1.7 kHz, both emission distributions gradually rise and then fall in frequency with local time; this is consistent with the ionospheric entry region of the waves remaining at a constant set of local times and latitudes over the course of the Earth’s rotation. Since higher frequencies in the TEM mode suffer greater attenuation while propagating in the E-I waveguide than do lower frequencies, the emissions’ highest frequency components will only be visible when Palmer’s local time is coincident with the local time of the emissions’ ionospheric penetration. As the Earth continues to rotate past this point, Palmer move further away from the ionospheric entry region for the emissions, and increased attenuation for high frequencies becomes apparent.

[32] There are also “chorus with hiss” emission components propagating in higher-order modes observed above the 1.7 kHz cutoff frequency between 0400 and 0800 MLT. These emissions extend less broadly in time than the main low-frequency peak of “chorus with hiss” emissions. It is not clear whether this is the result of a propagation effect (either attenuation within the Earth-ionosphere waveguide, or suffered during penetration of the ionosphere), or a source effect. The higher frequencies of “chorus with hiss” emissions are typically where hiss is observed, while chorus is observed at the lower frequencies.

[33] Observed “hiss only” emissions also display an upper frequency component, above the 1.7 kHz cutoff, which increases in frequency from 1.7 to ~ 4 kHz over the course of the emission interval, as has been seen before in previous work [e.g., *Vershinin*, 1970; *Carpenter et al.*, 1975]. The rising frequency of the upper component is

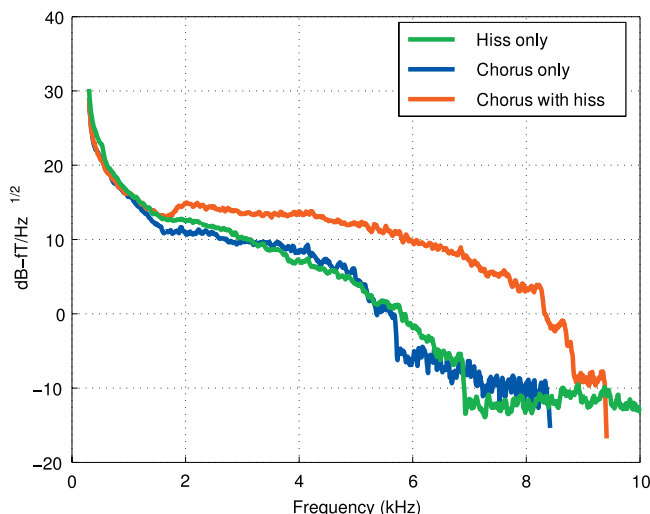


Figure 6. Cumulative emission spectra.

apparent, despite the nonlinear attenuation effects introduced by propagation in the Earth-ionosphere waveguide, which cause the upper frequency component to appear to “separate” from the lower frequency component of the hiss. Hayakawa *et al.* [1988] specifically interpreted the pre-midnight frequency drift of hiss in terms of a quasi-linear electron cyclotron instability model.

[34] The average spectra of the three emission types are shown in Figure 6. Note that the amplitude scale of the spectra of Figure 6 is not directly comparable to that of the cumulative spectrograms of Figure 5, because it is computed in a different way. The spectra of Figure 6 is computed by averaging the power spectra of all emissions of a given type. In this way, it provides a measure of the average power spectrum when an emission is present. This is in contrast to the average power spectrum at all times (including quiet periods), as in Figure 5, which also incorporates the occurrence probability at the given time and frequency.

[35] The characteristic rapid attenuation with increasing frequency of the TEM mode in the E-I waveguide is visible in Figure 6 for frequencies below 1.7 kHz. Above 1.7 kHz, the wave energy is contained in higher-order modes. “Chorus only” emissions extend up to approximately 5 kHz, “hiss only” emissions extend to 7 kHz and “chorus with hiss” emissions can be seen just beyond 8 kHz. It is important to note that, although some emissions may have high-frequency components, the likelihood of seeing any given emission type rapidly drops off with increasing frequency, as shown in a plot of emission occurrence versus frequency in Figure 7.

[36] These results are particularly interesting in the context of currently accepted definitions of midlatitude and plasmaspheric hiss. Specifically, Sonwalkar [1995] states that midlatitude hiss, which has a lower cutoff of ~ 2 kHz, is the only type of hiss visible on the ground at midlatitude stations like Palmer (contrasted with auroral hiss, which is visible at high-latitude ground stations). Plasmaspheric hiss, which occupies the portion of the hiss spectrum below ~ 2 –3 kHz is said not to be visible on the ground. However, as Figures 6 and 7 show, “hiss only” is readily seen at Palmer from 300 Hz (the peak of the spectrum) to nearly

7 kHz. This suggests one of three scenarios: (1) that midlatitude hiss may in fact extend below 3 kHz, (2) that plasmaspheric hiss, as well as midlatitude hiss, can penetrate to the ground at midlatitudes, in contrast to the prevailing belief that observations of plasmaspheric hiss are confined to space-based measurements, or (3) that the dusk hiss at Palmer represents an entirely different type of hiss, such as exo-hiss.

3.2. Occurrence Rates and Correlation With AE

[37] The appearance of chorus and hiss has long been known to correlate with the occurrence of substorms, as measured by the Auroral Electrojet (AE) index [Sazhin and Hayakawa, 1992; Hayakawa and Sazhin, 1992, and references therein]. When investigating the dependence of emission occurrence on AE, we look for emissions occurring during their usual “emission intervals,” as determined by Figure 5. For “chorus only” and “chorus with hiss,” we define the emission interval to be between 0300 and 0900 MLT. For “hiss only,” we define the emission interval to be between 1400 and 2300 MLT. We define the AE^\dagger index to be the maximum value of the true AE index in the 6 h preceding the center of the given emission’s emission interval. This is analogous to the definition for AE^* from [Meredith *et al.*, 2004], which is defined as the maximum value of AE in the 3 h prior to the emission; we elect to use AE^\dagger over AE^* , because we found that it is better correlated with our ground-based data. Figure 8 shows the normalized occurrence rates of “chorus only,” “hiss only” and “chorus with hiss” with respect to AE^\dagger .

[38] Consistent with past results, all three emission types generally increase in probability as AE^\dagger increases. The AE^\dagger dependence of “chorus only” contrasts with that of “chorus with hiss,” the latter being the most strongly AE^\dagger associated emission type. In particular, we note that when $AE^\dagger > 500$ nT, we see “chorus with hiss” more often than “chorus only,” and nearly twice as often when $AE^\dagger > 800$ nT. Because we know from Figure 5 that “chorus only” and “chorus with hiss” share the same local time emission interval, this further suggests that “chorus only” and “chorus with hiss” are in fact two manifestations of the

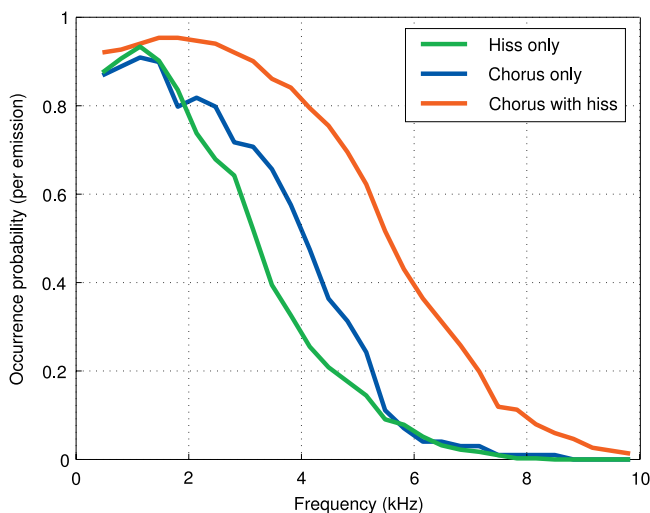


Figure 7. Cumulative occurrence probability (per emission) as a function of frequency.

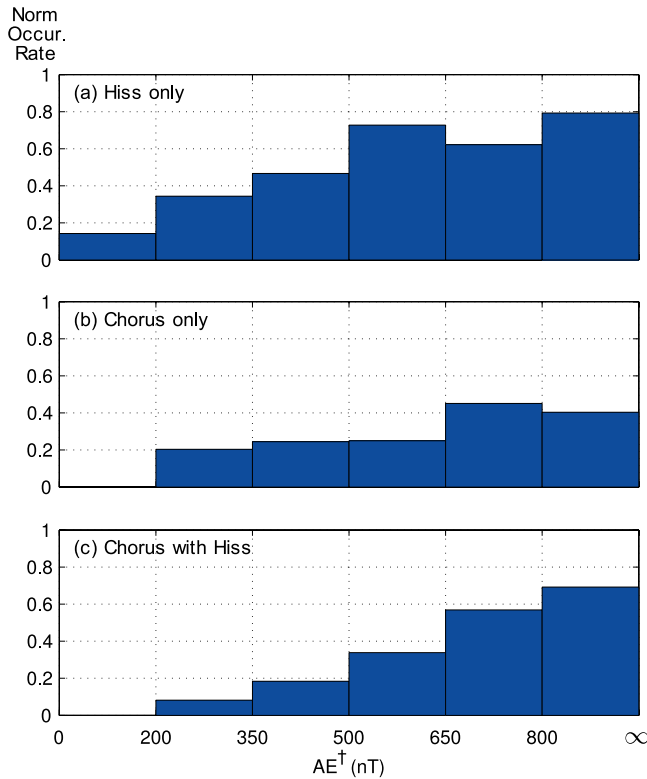


Figure 8. Dependence of (a) “hiss only,” (b) “chorus only,” and (c) “chorus with hiss” on AE^{\dagger} index. All bins have at least 35 days of data (mean number of days is 51, st. dev. is 10).

same chorus-producing phenomena, which has a tendency to induce hiss alongside the chorus when the AE index is increasingly disturbed. “Hiss only” occurrence is also well correlated with increasing values of AE^{\dagger} , and it is further interesting to note that “hiss only” is the only emission seen during the lowest levels of substorm activity, $AE^{\dagger} < 200$ nT.

[39] Figure 9 shows all emission types combined into a single cumulative spectrogram, and as a function of the AE^{\dagger} index. We show all emissions for all values of AE^{\dagger} , as well as all emissions for $AE^{\dagger} < 600$ nT and all emissions for $AE^{\dagger} > 700$ nT. The split point of $AE^{\dagger} = 650$ nT was chosen because that is the value for which there is an equal number of emissions above and below it (289 emissions for $AE^{\dagger} < 600$ nT and 288 emissions for $AE^{\dagger} > 700$ nT, respectively). We do not plot emissions for $600 \text{ nT} \leq AE^{\dagger} \leq 700 \text{ nT}$ because we assume that their characteristics will be very similar. The small, but visible discontinuity in Figures 9b and 9c at ~ 2000 MLT is an artifact of our processing; it appears because midnight UTC occurs at 1959 MLT, where one Palmer-generated spectrogram ends and another begins (as in Figure 2).

[40] We note from Figure 9 that the higher frequencies of “chorus with hiss” emissions (above ~ 1.7 kHz) tend to appear more frequently and at higher intensity for $AE^{\dagger} > 700$ nT. In general, when observing “chorus with hiss” emissions, the energy at higher frequencies is often composed primarily of hiss. The lack of energy at higher frequencies in Figure 9b indicates that chorus appears

without hiss at lower AE^{\dagger} levels, and with hiss at higher AE^{\dagger} levels, consistent with the above result from Figure 8.

[41] “Hiss only” emissions are also susceptible to changing geomagnetic conditions, in a very different way. At lower levels of AE^{\dagger} , we find that “hiss only” emissions extend from approximately 1400 to just past midnight MLT, and have very intense amplitude at lower ELF frequencies ($f < 500$ Hz). In contrast, for high AE^{\dagger} levels, the lower frequency ELF components of hiss are reduced, and the local time occurrence moves earlier, to 1000 to 2200 MLT. This result is in contrast to that of *Meredith et al.* [2006, section 6.3], who found no geomagnetic control of hiss on the nightside. However, we note that *Meredith et al.* [2006] divided day and night at 1800 MLT, which is near the middle of the dusk hiss peak at Palmer; separately analyzing the two halves of the hiss peak may have reduced the efficacy of their analysis. Nonetheless, there is obvious geomagnetic control in Figure 9 of dusk hiss after 1800 MLT (during *Meredith et al.*’s [2006] “night”).

4. Discussion

[42] Our results show two distinct types of hiss that are observed at Palmer, which we will refer to as “dawn hiss” and “dusk hiss.” Dawn hiss is observed exclusively in the dawn sector, is generally (but not exclusively) seen above ~ 2 kHz, often shows structure, and is always accompanied by chorus. In contrast, dusk hiss is observed exclusively in the dusk sector, is rarely seen above ~ 4 kHz, rarely shows structure, and is never observed with chorus. The frequency spectrum of dawn hiss observed at Palmer most closely resembles that of midlatitude hiss, while the spectrum of dusk hiss at Palmer resembles that of either plasmaspheric hiss or exo-hiss.

4.1. Chorus as a Source of Hiss

[43] That chorus and hiss are often observed together is a concept that is by no means novel. What is currently a new idea is that chorus may in fact be the dominant source of hiss, and that the one becomes the other via an overlapping and “smearing” of the spectrum, thus causing chorus emissions to lose the definition of their discrete elements, and eventually appear hiss-like to observers. *Santolik et al.* [2006] and *Bortnik et al.* [2008] have separately stated, on the basis of ray tracing studies, that chorus may be the primary source of ELF hiss and plasmaspheric hiss, respectively.

[44] The many observations of chorus emissions occurring simultaneously with hiss emissions, both in past works and in this paper, give credence to the claim that chorus may indeed be responsible for generating certain types of hiss. In particular, it seems quite reasonable that the dawn hiss shown in this paper, whose frequency band resembles midlatitude hiss, could be generated by discrete chorus emissions. The exclusive occurrence of dawn hiss with dawn chorus, and the fact that dawn hiss is so often of the “structured hiss” variety, both support the idea that midlatitude hiss may be caused by chorus.

[45] The most common variety of “chorus with hiss” seen at Palmer consists of one band of chorus at a lower frequency and one band of hiss at a higher frequency (although other varieties, such as overlapping bands of

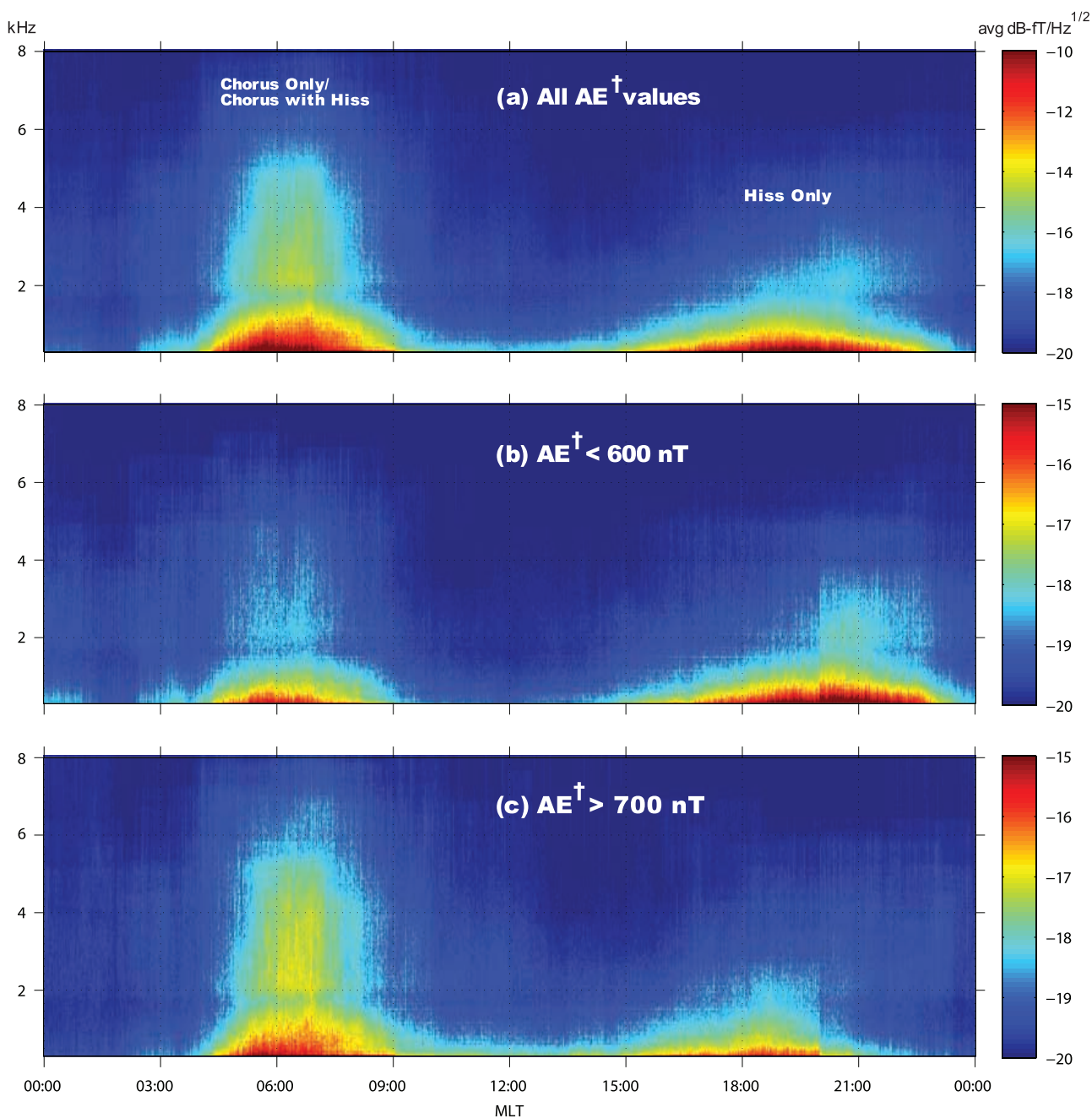


Figure 9. Cumulative spectrogram of (a) all chorus and hiss emissions (660 events), (b) all emissions for $AE^{\dagger} < 600$ nT (289 events), and (c) $AE^{\dagger} > 700$ nT (288 events). “Chorus only” and “chorus with hiss” are observed exclusively on the dawnside, while “hiss only” is observed exclusively on the duskside. AE^{\dagger} affects frequency occurrence for all emissions and the local time occurrence for “hiss only” emissions.

chorus and hiss, or bands of hiss below bands of chorus are possible). Although it is not reasonable to claim that chorus in one frequency band may be the source of simultaneously observed hiss in a separate band, it is certainly possible that chorus, originally occurring in multiple frequency bands, has either had one of its bands generated with hiss-like structure, or has had that band converted into hiss over the course of its propagation. The former scenario is supported by the observations of *Cornilleau-Wehrin et al.* [1978], who made many observations of “chorus with hiss” beyond the plasmopause, presumably close to the source region,

which suggests that the conversion process happens very close to, or at, the source. However, the latter scenario is supported by *Santolik et al.* [2006] and *Bortnik et al.* [2008], who suggest that chorus waves may convert to hiss via superposition and dispersion during their propagation. It is not clear at this time which conversion process is dominant.

[46] The fact that we usually see hiss or structured hiss in a band above chorus, coupled with the fact that chorus frequency tracks the electron gyrofrequency at its source region [Burtis and Helliwell, 1976], suggests that it may

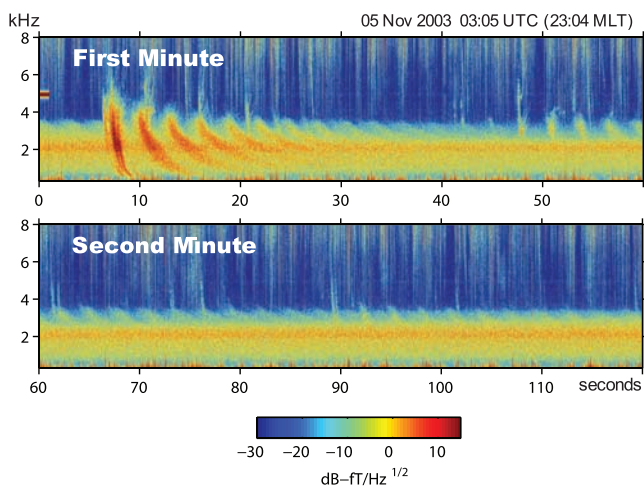


Figure 10. A multiply-hopping whistler, whose multitude of cross-hemisphere hops gradually overlap with an existing hiss band. (top) The original whistler is seen in the first minute, and quickly merges with the existing hiss band, becoming (bottom) indistinguishable from standard structureless hiss in the second minute. This type of phenomenon supports the idea that dusk hiss observed at Palmer may be caused by lightning.

specifically be chorus generated at lower L shells (where the equatorial electron gyrofrequency is higher) that gives rise to hiss, whereas chorus generated at higher L shells (where the equatorial electron gyrofrequency is lower) remain structured as chorus. Again, this conversion process may occur either at the source, or during the chorus propagation. If the conversion occurs during chorus propagation, it is possible that the conversion region is small; this fact would not preclude chorus generated at low L shells from being favored to convert over chorus generated at higher L shells, despite the fact that chorus generated at low L shells has a shorter distance to travel before it reaches the ionosphere.

[47] As seemingly plausible as it is that dawn hiss is caused by chorus, it seems equivalently unlikely that the dusk hiss observed at Palmer is related to chorus. The fact that very few emissions are seen at Palmer in between the diurnal peaks of dawn “chorus only”/“chorus with hiss” and dusk “hiss only,” as well as the lack of structure in dusk hiss emissions, strongly suggest that the emissions that occur at these two separate local times are unrelated. It is also quite unlikely that chorus, being observed very infrequently in the dusk sector in situ [Tsurutani and Smith, 1977; Meredith et al., 2001], could propagate azimuthally from the dawn to the dusk sector before being observed as hiss; the ray tracing studies of Santolik et al. [2006], in particular, show a negligible amount of azimuthal cross-field line propagation. Whether dusk hiss is exo-hiss or plasmaspheric hiss, past studies of the local time distribution of chorus, as well as chorus observations from this study, do not support the hypothesis that dusk hiss is generated by magnetospheric chorus.

4.2. Lightning as a Source of Hiss

[48] There has recently been a resurgence of interest in the role of lightning as a source of plasmaspheric hiss, either

embryonically, as proposed by Sonwalkar and Inan [1989] or as a result of multiple magnetospheric reflections within the plasmasphere, as proposed by Draganov et al. [1992]. Green et al. [2005] suggested that lightning is the dominant source of plasmaspheric hiss over the frequency range of ~ 500 Hz to 3 kHz, though the particular frequency range was contested by a subsequent study by Meredith et al. [2006], who concluded that the lightning-associated hiss was limited to frequencies above 2 kHz.

[49] The local time peak of dusk hiss at Palmer is suggestive of afternoon lightning as a source. Particularly compelling is the fact that dusk hiss peaks at Palmer at around 1900 MLT, which corresponds to 1700–1800 MLT for the Eastern half of North America, a major source of lightning during the boreal summer [Christian et al., 2003]. This local time peak is quite close to the ~ 1600 MLT peak of lightning worldwide (e.g., J. C. Bailey et al., Diurnal lightning distributions as observed by the optical transient detector (otd) and the lightning imaging sensor (lis), paper presented at 13th International Conference on Atmospheric Electricity, Chinese Academy of Sciences, Beijing, 13–17 August 2007). The ~ 2 -h discrepancy between the diurnal peaks of terrestrial lightning and dusk hiss at Palmer may be an ionospheric effect, since ionospheric absorption is greater during daylight hours than at night [e.g., Helliwell, 1965, Figure 3–31]; this would have the artificial effect of damping observed hiss amplitudes during the daytime. Although seasonal results are by no means conclusive for a single year of data, it is worth noting that we see dusk hiss in its usual emission interval at Palmer (1400–2300 MLT) on 3.5 times as many days in June, July and August than in January, February and March 2003 (124 versus 34 days); this is consistent with the boreal summer peak of North American lightning.

[50] Whistlers can be seen quite often at Palmer, varying from a peak of 22 whistlers per minute during the boreal summer (local winter) night, to a minimum of 0.3 whistlers per minute during the day in the boreal winter, according to calculations by Burgess [1993], based on earlier audio recording measurements by Laaspere et al. [1964] at a nearby Antarctic station. We also occasionally see evidence of whistlers directly causing or contributing to bands of hiss at Palmer. Figure 10 shows an example of a whistler undergoing many cross-hemisphere hops, merging with an existing hiss band. Over the course of the 2 min shown in Figure 10, the whistler, at first highly visible on the spectrogram, completely merges with the hiss and becomes indistinguishable from unstructured hiss at the end of the second minute. Although this phenomenon is not seen very often at Palmer, the lack of observations may be due to fact that the “triggering” mechanism of the whistler lasts for such a short amount of time. We hypothesize that these multiply-hopping whistlers may contribute to the dusk hiss at Palmer, either as the result of many overlapping, dispersed whistlers [e.g., Dowden, 1971], or possibly in conjunction with the type of embryonic onset reported by Sonwalkar and Inan [1989]. However, until either more cases can be found that show evidence of triggering onset, or until the absence of such observations can be theoretically explained, we cannot suggest that these particular mechanisms of whistler-induced hiss are the dominant source of dusk hiss.

[51] It is also important to note that the low frequency peak (<300 Hz) of dusk hiss is inconsistent with lightning control as determined by both *Green et al.* [2005] and *Meredith et al.* [2006], who found no evidence of lightning control below 500 Hz and 2 kHz, respectively. However, we must critically interpret their conclusions. If these lower-frequency waves were caused by terrestrial lightning flashes, then certain propagation effects would make them inherently difficult to spatially correlate with their terrestrial source region. As noted by *Meredith et al.* [2006, p. 9], lower frequency waves are capable of propagating outward in the magnetosphere to L shells quite distant from their terrestrial source [*Bortnik et al.*, 2003]. Additionally, the lower attenuation for lower frequencies in the TEM mode in the Earth-ionosphere waveguide (particularly over seawater) allows waves to potentially propagate subionospherically very far from their source before leaking into the magnetosphere. Thus, we conclude that spatial correlation with landmass is not a requirement for lightning as the source of lower frequency waves. Finally, although we note from Figure 8 that “hiss only” emissions are well correlated with geomagnetic activity, this fact is not mutually exclusive with the theory that hiss is sourced by terrestrial lightning. *Sonwalkar and Inan* [1989], for example, hypothesized that lightning-generated whistlers are an embryonic source of plasmaspheric hiss, which suggests that a source population of energetic particles, such as those injected into the plasmasphere via magnetic storms, are still necessary for the growth of hiss to observable levels.

5. Summary

[52] Dawn hiss at Palmer is regularly observed with chorus, and may in fact be generated by chorus, either via diffuse generation at the chorus source region, or via an overlapping and smearing of the chorus frequency band over the course of the chorus propagation. Dusk hiss seen at Palmer, which is either exo-hiss, or unexpected ground-based observations of plasmaspheric hiss, appears to be consistent with the idea of lightning as a source, but is not consistent with chorus as a source. Significant work remains to determine the relation between hiss observed at Palmer and in space, and to conclusively determine the sources for the dawn and dusk hiss observed at Palmer.

[53] **Acknowledgments.** This work was supported by the NSF under grants ATM-0524805 and ANT-0538627 and by NASA under grant NNG04GN01G.

[54] Zuyin Pu thanks Ondrej Santolik and Vikas Sonwalkar for their assistance in evaluating this paper.

References

- Abel, B., and R. M. Thorne (1998), Electron scattering loss in Earth's inner magnetosphere: I. Dominant physical processes, *J. Geophys. Res.*, **103**, 2385–2396, doi:10.1029/97JA02919.
- Alcock, G. M. (1957), A study of the audio-frequency radio phenomenon known as “dawn chorus,” *Aust. J. Phys.*, **10**, 286–298.
- Bortnik, J., U. S. Inan, and T. F. Bell (2003), Energy distribution and lifetime of magnetospherically reflecting whistlers in the plasmasphere, *J. Geophys. Res.*, **108**(A5), 1199, doi:10.1029/2002JA009316.
- Bortnik, J., R. M. Thorne, and N. P. Meredith (2008), The unexpected origin of plasmaspheric hiss from discrete chorus emissions, *Nature*, **452**, 62–66, doi:10.1038/nature06741.
- Burgess, W. C. (1993), Lightning-induced coupling of the radiation belts to geomagnetically conjugate ionospheric regions, Ph.D. thesis, Stanford Univ., Stanford, Calif.

- Burtis, W. J., and R. A. Helliwell (1976), Magnetospheric chorus: Occurrence patterns and normalized frequency, *Planet. Space Sci.*, **24**, 1007–1007, doi:10.1016/0032-0633(76)90119-7.
- Carpenter, D. L., J. C. Foster, T. J. Rosenberg, and L. J. Lanzerotti (1975), A subauroral and mid-latitude view of substorm activity, *J. Geophys. Res.*, **80**, 4279–4286.
- Christian, H. J., et al. (2003), Global frequency and distribution of lightning as observed from space by the Optical Transient Detector, *J. Geophys. Res.*, **108**(D1), 4005, doi:10.1029/2002JD002347.
- Chum, J., and O. Santolik (2005), Propagation of whistler-mode chorus to low altitudes: Divergent ray trajectories and ground accessibility, *Ann. Geophys.*, **23**, 3727–3738.
- Cornilleau-Wehrin, N., R. Gendrin, F. Lefeuvre, M. Parrot, R. Gard, D. Jones, A. Bahnsen, E. Ungstrup, and W. Gibbons (1978), VLF electromagnetic waves observed onboard GEOS-1, *Space Sci. Rev.*, **22**, 371–382.
- Dowden, R. L. (1971), Distinctions between mid latitude VLF hiss and discrete emissions, *Planet. Space Sci.*, **19**, 374–376, doi:10.1016/0032-0633(71)90100-0.
- Draganov, A. B., U. S. Inan, V. S. Sonwalkar, and T. F. Bell (1992), Magnetospherically reflected whistlers as a source of plasmaspheric hiss, *Geophys. Res. Lett.*, **19**, 233–236.
- Dunckel, N., and R. A. Helliwell (1969), Whistler-mode emissions on the OGO 1 satellite, *J. Geophys. Res.*, **74**, 6371–6385, doi:10.1029/JA074i026p06371.
- Green, J. L., S. Boardsen, L. Garcia, W. W. L. Taylor, S. F. Fung, and B. W. Reinisch (2005), On the origin of whistler mode radiation in the plasmasphere, *J. Geophys. Res.*, **110**, A03201, doi:10.1029/2004JA010495.
- Gurnett, D. A., and T. B. Burns (1968), The low-frequency cutoff of ELF emissions, *J. Geophys. Res.*, **73**, 7437–7445, doi:10.1029/JA073i023p07437.
- Hayakawa, M., and S. S. Sazhin (1992), Mid-latitude and plasmaspheric hiss—A review, *Planet. Space Sci.*, **40**, 1325–1338, doi:10.1016/0032-0633(92)90089-7.
- Hayakawa, M., Y. Tanaka, and J. Ohtsu (1975a), The morphologies of low-latitude and auroral VLF ‘hiss,’ *J. Atmos. Terr. Phys.*, **37**, 517–529.
- Hayakawa, M., Y. Tanaka, and J. Ohtsu (1975b), Satellite and ground observations of magnetospheric VLF hiss associated with the severe magnetic storm on May 25–27, 1967, *J. Geophys. Res.*, **80**, 86–92.
- Hayakawa, M., K. Bullough, and T. R. Kaiser (1977), Properties of storm-time magnetospheric VLF emissions as deduced from the Ariel 3 satellite and ground-based observations, *Planet. Space Sci.*, **25**, 353–368, doi:10.1016/0032-0633(77)90051-4.
- Hayakawa, M., Y. Tanaka, and T. Okada (1985), Morphological characteristics and the polarization of plasmaspheric ELF hiss observed at Moshiri ($L \sim 1.6$), *J. Geophys. Res.*, **90**, 5133–5140.
- Hayakawa, M., Y. Tanaka, T. Okada, M. Tixier, and S. S. Sazhin (1988), Substorm-associated VLF emissions with frequency drift observed in the premidnight sector, *J. Geophys. Res.*, **93**, 5685–5700.
- Helliwell, R. A. (1965), *Whistlers and Related Ionospheric Phenomena*, Stanford Univ. Press, Stanford, Calif.
- Helliwell, R. A., D. L. Carpenter, U. S. Inan, and J. P. Katsufakis (1986), Generation of band-limited VLF noise using the Siple transmitter: A model for magnetospheric hiss, *J. Geophys. Res.*, **91**, 4381–4392, doi:10.1029/JA091iA04p04381.
- Horne, R. B., S. A. Glauert, and R. M. Thorne (2003), Resonant diffusion of radiation belt electrons by whistler-mode chorus, *Geophys. Res. Lett.*, **30**(9), 1493, doi:10.1029/2003GL016963.
- Horne, R. B., et al. (2005), Wave acceleration of electrons in the Van Allen radiation belts, *Nature*, **437**, 227–230, doi:10.1038/nature03939.
- Jørgensen, T. S. (1968), Interpretation of auroral hiss measured on OGO 2 and at Byrd Station in terms of incoherent Cerenkov radiation, *J. Geophys. Res.*, **73**, 1055–1069, doi:10.1029/JA073i003p01055.
- Kleimenova, N. G., M. S. Kovner, and V. A. Kuznetsova (1976), VLF-ground observations near the plasmapause projections, *J. Atmos. Terr. Phys.*, **38**, 1215.
- Koons, H. C. (1981), The role of hiss in magnetospheric chorus emissions, *J. Geophys. Res.*, **86**, 6745–6754.
- Laaspere, T., M. Morgan, and W. Johnson (1964), Chorus, hiss, and other audio-frequency emissions at stations of the whistlers-east network, *Proc. IEEE*, **52**(11), 1331–1349.
- Lyons, L. R., and R. M. Thorne (1973), Equilibrium structure of radiation belt electrons, *J. Geophys. Res.*, **78**, 2142–2149, doi:10.1029/JA078i013p02142.
- Lyons, L. R., R. M. Thorne, and C. F. Kennel (1972), Pitch-angle diffusion of radiation belt electrons within the plasmasphere, *J. Geophys. Res.*, **77**, 3455–3474.
- Maeda, K. (1962), Whistlers and VLF emissions in connection with the Earth storm, *J. Phys. Soc. Jpn.*, **17**, suppl., B95.

- Makita, K. (1979), VLF-LF hiss emissions associated with the aurora, *Mem. Natl. Inst. Polar Res., Ser. A*, 16.
- Meredith, N. P., R. B. Horne, and R. R. Anderson (2001), Substorm dependence of chorus amplitudes: Implications for the acceleration of electrons to relativistic energies, *J. Geophys. Res.*, 106, 13,165–13,178, doi:10.1029/2000JA900156.
- Meredith, N. P., R. B. Horne, R. M. Thorne, D. Summers, and R. R. Anderson (2004), Substorm dependence of plasmaspheric hiss, *J. Geophys. Res.*, 109, A06209, doi:10.1029/2004JA010387.
- Meredith, N. P., R. B. Horne, M. A. Clilverd, D. Horsfall, R. M. Thorne, and R. R. Anderson (2006), Origins of plasmaspheric hiss, *J. Geophys. Res.*, 111, A09217, doi:10.1029/2006JA011707.
- Parady, B. K., D. D. Eberlein, J. A. Marvin, W. W. L. Taylor, and L. J. Cahill Jr. (1975), Plasmaspheric hiss observations in the evening and afternoon quadrants, *J. Geophys. Res.*, 80, 2183–2198.
- Parrot, M., O. Santolik, D. Gurnett, J. Pickett, and N. Cornilleau-Wehrin (2004), Characteristics of magnetospherically reflected chorus waves observed by CLUSTER, *Ann. Geophys.*, 22, 2597–2606.
- Pope, J. H. (1957), Diurnal variation in the occurrence of 'dawn chorus,' *Nature*, 180, 433, doi:10.1038/180433a0.
- Pope, J. H. (1960), Effect of latitude on the diurnal maximum of 'dawn chorus,' *Nature*, 185, 87–88, doi:10.1038/185087b0.
- Russell, C. T., R. L. McPherron, and P. J. Coleman Jr. (1972), Fluctuating magnetic fields in the magnetosphere. I: ELF and VLF fluctuations, *Space Sci. Rev.*, 12, 810–856, doi:10.1007/BF00173072.
- Santolik, O. (2008), New results of investigations of whistler-mode chorus emissions, *Nonlinear Processes Geophys.*, 15, 621–630.
- Santolik, O., J. Chum, M. Parrot, D. A. Gurnett, J. S. Pickett, and N. Cornilleau-Wehrin (2006), Propagation of whistler mode chorus to low altitudes: Spacecraft observations of structured ELF hiss, *J. Geophys. Res.*, 111, A10208, doi:10.1029/2005JA011462.
- Sazhin, S. S., and M. Hayakawa (1992), Magnetospheric chorus emissions—A review, *Planet. Space Sci.*, 40, 681–697, doi:10.1016/0032-0633(92)90009-D.
- Sonwalkar, V. S. (1995), *Handbook of Atmospheric Electrodynamics, vol. II*, pp. 407–460, CRC Press, Boca Raton, Fla.
- Sonwalkar, V. S., and J. Harikumar (2000), An explanation of ground observations of auroral hiss: Role of density depletions and meter-scale irregularities, *J. Geophys. Res.*, 105, 18,867–18,884, doi:10.1029/1999JA000302.
- Sonwalkar, V. S., and U. S. Inan (1989), Lightning as an embryonic source of VLF hiss, *J. Geophys. Res.*, 94, 6986–6994.
- Spasojevic, M., and U. S. Inan (2005), Ground based VLF observations near $L = 2.5$ during the Halloween 2003 storm, *Geophys. Res. Lett.*, 32, L21103, doi:10.1029/2005GL024377.
- Storey, L. R. O. (1953), An investigation of whistling atmospherics, *Philos. Trans. R. Soc. London, Ser. A*, 246, 113–141.
- Taylor, W. W. L., and D. A. Gurnett (1968), Morphology of VLF emissions observed with the Injun 3 satellite, *J. Geophys. Res.*, 73, 5615–5626.
- Thorne, R. M., and C. F. Kennel (1967), Quasi-trapped VLF propagation in the outer magnetosphere, *J. Geophys. Res.*, 72, 857–870.
- Thorne, R. M., E. J. Smith, R. K. Burton, and R. E. Holzer (1973), Plasmaspheric hiss, *J. Geophys. Res.*, 78, 1581–1596, doi:10.1029/JA078i010p01581.
- Tsurutani, B. T., and E. J. Smith (1974), Postmidnight chorus: A substorm phenomenon, *J. Geophys. Res.*, 79, 118–127, doi:10.1029/JA079i001p00118.
- Tsurutani, B. T., and E. J. Smith (1977), Two types of magnetospheric ELF chorus and their substorm dependences, *J. Geophys. Res.*, 82, 5112–5128.
- Vershinin, E. F. (1970), About the intensity of the hiss near inner boundary of the plasmopause and about the bursts of hiss with drifting frequency, *Ann. Geophys.*, 26, 703.

D. I. Golden, U. S. Inan, and M. Spasojevic, Space, Telecommunications, and Radioscience Laboratory, Stanford University, 350 Serra Mall, Packard Building, Room 351, Stanford, CA 94305, USA. (dgolden1@stanford.edu)